RMK 42

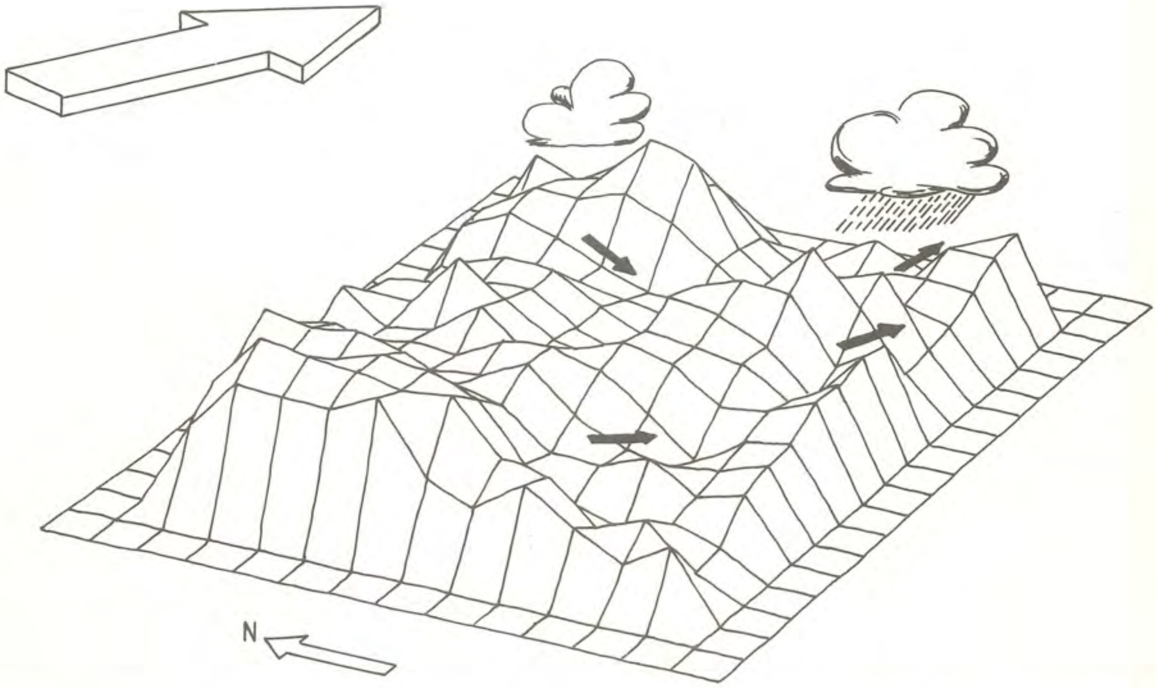

ESTIMATION OF OROGRAPHIC PRECIPITATION BY DYNAMICAL INTERPRETATION OF SYNOPTIC MODEL DATA

by Stefan Gollvik

SMHI SWEDISH METEOROLOGICAL AND HYDROLOGICAL INSTITUTE

SMHI Reports
Meteorology and Climatology

RMK 42

ESTIMATION OF OROGRAPHIC PRECIPITATION BY DYNAMICAL INTERPRETATION OF SYNOPTIC MODEL DATA

by Stefan Gollvik

This project has been financed by the Swedish Association of River Regulation Enterprises (VASO)

SMHI:s tryckeri 1984

Issuing Agency SMHI S-60176 Norrköping Sweden	Report number RMK 42 Report date November 1984

Author (s)

Stefan Gollvik

Title (and Subtitle)

Estimation of orographic precipitation by dynamical interpretation of synoptic model data

Abstract

A dynamical model for computing orographic precipitation, which utilizes a large-scale numerical model and information about local orography, has been developed. Some cloud physics is incorporated in the model. The precipitation is strongly dependent on the estimation of the vertical velocity. The model has been tested for a three month period and compared with observations. The problem of verification is also discussed.

Key words

Orographic precipitation
Dynamical interpretation

Supplementary notes	Number of pages	Language
	20	English

ISSN and title

0347-2116 SMHI Reports Meteorology and Climatology

Report available from:

LIST OF CONTENTS

1. INTRODUCTION

One problem in the field of numerical weather prediction (NWP) is to forecast the precipitation. The processes in nature that produce rain and snow are very complicated, and much work has been done in the field of cloud physics (e g Mason, 1971). When it comes to forecasting in numerical weather prediction models, many simplifications have to be done. The resolution of the models, used for weather forecasts is normally of more than 100 km between the grid-points but the variations of humidity and precipitation have often a much smaller horizontal scale. The main reason for including humidity in NWP-models is to get a proper dynamical development caused partly by the release of latent heat. The condensed water, produced in the models, is usually assumed to rain out immediately due to the problems of including a cloud phase. It is, however, a too simple treatment for making good forecasts of the precipitation. Some work has been done, where the cloud water density is a dependent variable in the model, but it has not yet been used in routine forecasts (Sundqvist, 1981). A better treatment of clouds is important also for interaction with the radiation scheme of the model.

We know that the airflow and hence the precipitation pattern is strongly affected by local orography. We also know that the airflow on the meso-scale interacts back to the large-scale flow. Here we neglect the latter and assume that, as a first approximation, the precipitation pattern can be determined by information of the large-scale flow (i e a numerical forecast) and of local orography. This means that we do a dynamical interpretation of the forecast at different times, but the result of this does not affect the evolution of the large-scale forecast.

The present paper is based mainly on an earlier work by Bell (1978), but substantial modifications are done in the dynamics, by utilizing another model, for computing a two-dimensional wind field in the lowest layer (Danard, 1977, Olsson, 1984).

2. METHOD DESCRIPTION

We have used the Swedish limited area model, LAM, (Undén, 1982) as the large-scale model. The values from LAM are taken every third hour from +12h to +36h, and the method can be described as follows:

1. Interpolate the values of wind, vertical velocity, temperature, geopotential and humidity, at different levels, from the large-scale model grid, to a small-scale ($\Delta x \sim 5$ km) computation grid.

2. Utilize the information about orography on that scale and estimate how the air is displaced vertically, to see where saturation is reached. Also compute the vertical velocity field, as modified by orography.

3. Use the estimated vertical velocity to compute the precipitation rate.

4. Modify the precipitation rate by washout, i e the precipitation from a layer is enhanced by coalescence. Also estimate how the evaporation in unsaturated layer is modifying the precipitation.

3. HORIZONTAL INTERPOLATION

The problem is to estimate the values of the large-scale model in an arbitrary point. We have used bi-linear interpolation, which is assumed to be good enough, for this application. There are no special problems in the free atmosphere, but some considerations have to be done in the case where the orography of the large-scale model intersects the pressure surface, on to which the actual variable is to be interpolated. We start with values of the large-scale model at every 100th mb as well as surface values of pressure, two-meter temperature and humidity and ten-meter winds. The latter values are computed using the parameterisation of the layer fluxes in the large-scale model, (Businger et al., 1971, Paulson, 1970). The interpolation, to a point C, is done in the following way (see Figure 1), using the information in the two points A and B:

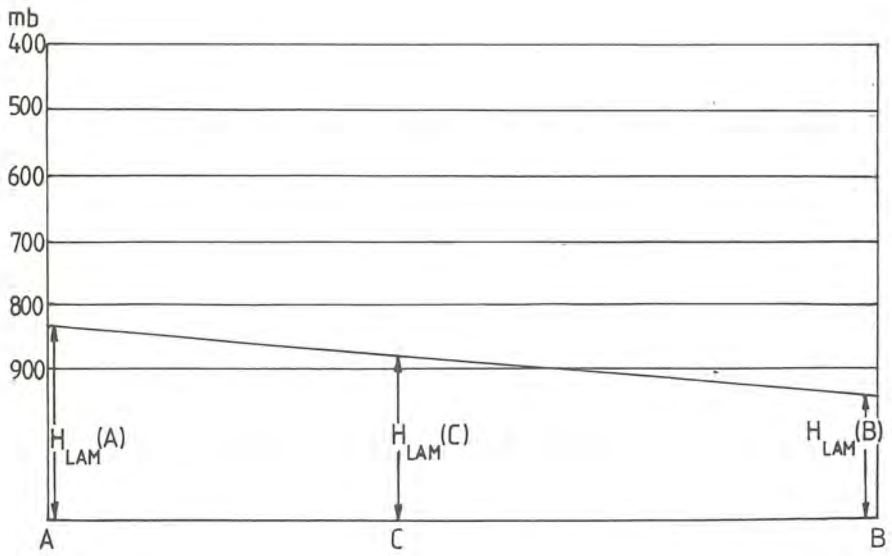

Figure 1 **Horizontal interpolation.**

i) Interpolate the large-scale model orography H_{LAM} linearly to the point C, $H_{LAM}(C)$.

ii) Also do a linear interpolation of surface parameters, i e surface pressure (p_s), two meter temperature and humidity (T_s and q_s) and ten meter wind (V_s). The large-scale vertical velocity $\omega_{LAM} = \frac{dp}{dt}_{LAM}$ is assumed to be zero at the surface. This should not be too serious, since the slope of the large-scale orography is much smaller than that of the small-scale orography.

iii) The values in the free atmosphere are also interpolated, but for the variables at a pressure which is below the surface at one point (900mb values in point A in the figure) we use the interpolation weights from the lowest not intersecting layer. In this case it means that the temperature at 900mb (T9) is computed according to:

$$T9(C) = T9(A) + \frac{CB}{AB} * (T8(A) - T8(B)) \qquad (3.1)$$

4. VERTICAL DISPLACEMENT

After the horizontal interpolation to the small-scale grid, we have the large-scale model values as they would be if no small-scale orography is present. We assume that the introduction of this orography implies a vertical displacement of the air. The model uses up to seven 100mb layers. The lowest layer and its thickness are determined from the surface pressure. The orographic uplift (H_T), is proportional to the difference between the height of the small-scale orography (H) and that of the large-scale model (H_{LAM}).

$$H_T = k_T(p) \cdot (H-H_{LAM}) \tag{4.1}$$

The parameter k_T varies linearly with height from 1 at the surface to 0 at 400 mb (see Figure 2).

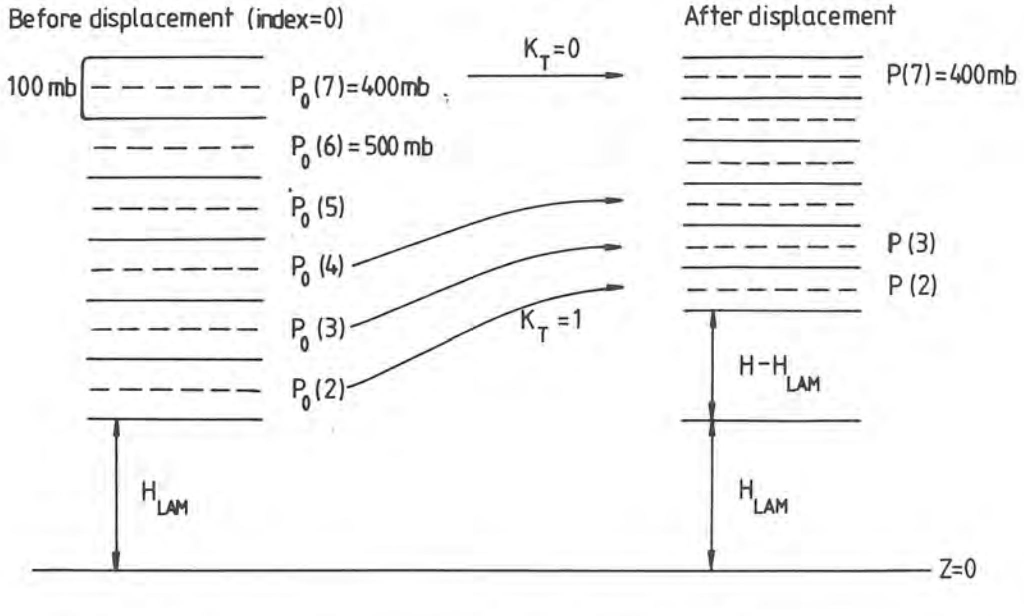

Figure 2 The parameterization of the orographic uplift.

When the air is lifted we assume a linear change in the relative humidity, U:

$$U = U_o(1+\alpha\, H_T) \tag{4.2}$$

where $\alpha = \frac{g}{R\,T_o}\left(\frac{\varepsilon}{C_p}\frac{L}{T_o} - 1\right)$

Here index zero refers to the values before the displacement, and g = acceleration of gravity, R = specific gas constant for air, ε = 0.622, L = latent heat of vaporization and C_p = specific heat at constant pressure.

The level at which we reach saturation (H_s) is computed by setting U = 1 in (4.2):

$$H_s = (1 - U_o)/\alpha U_o \qquad (4.3)$$

By utilizing (4.1)-(4.3) we compute, for each layer, modified values of pressure, temperature and humidity. In doing so we lift the air dry-adiabatically to the condensation level (H_s) and from H_s to H_T along a pseudo-adiabat.

5. VERTICAL VELOCITY

5.1 General discussion

In this model the precipitation rate is proportional to the vertical velocity (see section 6). Therefore the results of the model simulations, are very much dependent on the estimation of this quantity.

It is a very difficult problem to compute the vertical velocity field on the meso-scale. This is so, since this quantity (in a hydrostatic model) is derived from the divergence of the horizontal wind field.

One possible way would be to run a complete three-dimensional time-dependent meso-scale model from a detailed analysis. However, for the timescales of interest here, this means a much too large area of integration for all practical available computational possibilities. We instead assume that:

i) the meso-scale wind field is determined by the large-scale weather situation, and the forcing from the orography.

ii) The modification of the large-scale flow due to the small-scale flow is of minor importance. (Actually small-scale features should already be incorporated in the large-scale model, in the different schemes of physical parameterization, to give a proper evolution on the large-scale).

iii) The effects of the large-scale divergence and the small-scale divergence are linear, i e the vertical velocity can be regarded as a sum of the large-scale vertical velocity and that of the small-scale. We will then see that generally the small-scale divergence is dominating.

Assumption i) above means that we treat the meso-scale flow, not as a time-dependent problem, but rather as a steady state boundary value problem.

5.2 Model formulations

Here we have used two different ways of computing the orographically induced vertical velocity. Bell (1978) used the following formulation:

$$\omega_T(p) = - k_T(p) \cdot V_H(p) \cdot \nabla H \cdot g\rho \tag{5.2.1}$$

where $\omega_T = \frac{dp}{dt}$ is the small-scale vertical velocity and $k_T(p)$ is defined in section 4. The total vertical velocity is then given as

$$\omega(p) = \omega_T(p) + \omega_{LAM}(p) \tag{5.2.2}$$

where we have utilized assumption iii) above.

The disadvantage of this simple formulation is that we have no horizontal coupling of the vertical velocity field, i e the vertical velocity is determined by the local orographic gradients, regardless of the neighbouring points. The effect of stratification is neglected, and no air is allowed to blow around the mountains.

Therefore, we have also used another approach where we utilized a two-dimensional wind simulation model, developed by Danard (1977), and modified by Olsson (1984) for computing the wind in lower levels. This Small Area Model (SAM) utilizes the free atmosphere wind and temperature as input data, together with information about orography, roughness length (z_0) and estimated 2m-temperature on the small-scale orography. The result from a run with this model is a two-dimensional low level wind field, containing divergence, which can be interpreted as a small-scale vertical velocity in the boundary layer. A short description of this two-dimensional model is given in section 5.3.

In this case we instead of (5.2.2) use the following formulation:

$$\omega(p) = C(p) \cdot \omega_{SAM} + (1-C(p))\omega_T(p) + \omega_{LAM}(p) \tag{5.2.3}$$

Here ω_{SAM} is the boundary layer vertical velocity of the small area model and $C(p)$ has in the experiments been chosen to $k_T(p)$. By this formulation we utilize the wind information of the free atmosphere, and at the same time use ω_{SAM} as a lower boundary condition.

5.3 Small-Area Model

The small-area model (Danard, 1977, Olsson 1984) produces a two-dimensional meso-scale flow in the boundary layer, as a dynamical interpretation of the large-scale flow. This is done by a time integration starting with 'free atmospheric' data where the effects of stratification, orography, thermal forcing and surface friction, are included.

One parameter in this model is the boundary layer height (H_B), which here is a function of space only. By this assumption we have no free upper surface in the model and pressure changes are only dependent on temperature changes. One consequence of this is that the model does not contain gravity waves.

The governing equations are:

$$\frac{\partial \mathbb{V}}{\partial t} = - \mathbb{V} \cdot \nabla \mathbb{V} - (g \nabla H + RT_s \nabla \ell n p_s) - f k \times \mathbb{V} + F + Km \nabla^2 \mathbb{V} \tag{5.3.1}$$

$$\frac{\partial \ell n p_s}{\partial t} = - \frac{g}{R\Theta_s T_s} \int_0^{H_B} \frac{\partial \Theta}{\partial t} dz \tag{5.3.2}$$

$$\frac{\partial \Theta_s}{\partial t} = - \mathbb{V} \cdot \nabla \Theta_s + K_H \nabla^2 \Theta_s + Q \tag{5.3.3}$$

$$\frac{\partial \Theta}{\partial t} = \frac{\partial \Theta_s}{\partial t} \cdot f (H_B, V) \tag{5.3.4}$$

Here the notation is standard and index s refers to surface values. Surface friction is denoted by F, and K_m and K_H are diffusion coefficients. The diabatic heating term Q is important for the results of the run. The formulation of Q can be described as follows:

i) Compute the temperature at the earth surface (T_i) by an extrapolation from the values at 700 mb and 800mb.

ii) Estimate an 'undisturbed observed' temperature at the earth surface (T_o). When SAM is run from an analysis this value is chosen to be the observed temperature on a place near the actual place, where the effects of local circulation can be neglected. In this case, where we utilize a large-scale model, T_o is chosen as

$$T_o = T_{2met}(LAM) + \gamma (H-H_{LAM}) \tag{5.3.5}$$

where $\gamma = (T_{800mb}(LAM) - T_{2met}(LAM))/(Z_{800mb}(LAM) - H_{LAM})$ (5.3.6)

iii) Let the heating be proportional to the difference between these two temperatures, i e

$$Q = \frac{\Theta_s}{T_s} \cdot \frac{\Delta T}{\tau} \tag{5.3.7}$$

where $\Delta T = T_o - T_i$ and τ is the time, under which the diabatic effects are active. The time τ is chosen to be the actual forecast time of the model.

The initial state from which (5.3.1) to (5.3.4) is integrated is given by:

$\mathbb{V}$ = 900mb LAM-wind reduced by an Ekman-profile

$T = T_i$

P_s= Hydrostatically reduced pressure from 800mb height

After the integration we regard the wind field as an interpretation of the low level wind when the effects of small-scale orography and roughness are incorporated.

The divergence of this wind is used for computing the vertical velocity, where we assume that the divergence is zero at the height H_B. This assumption is consistant within this model. In reality we have an upper level divergence, giving another vertical velocity field. Actually the vertical velocity estimated from the model could be regarded as a tuning constant multiplied by the divergence. This has, however, not been utilized in this study. The effect of higher level divergence is included by the use of formula (5.2.3).

6. PRECIPITATION COMPUTATION

6.1 Production of precipitation

As mentioned in section 5 the rate, at which precipitation is produced, is proportional to the vertical velocity, ω:

$$P_1 = - k_1 \cdot k_2 \cdot \omega \cdot \frac{\partial q_s}{\partial p} \cdot \rho \cdot \Delta Z \qquad (6.1.1)$$

here P_1 is the precipitation rate ($kg \cdot m^{-2} \cdot s^{-1}$) k_1 and k_2 are physical parameters (see below), ΔZ is the layer thickness, and $\frac{\partial q_s}{\partial p}$ is the variation of saturation mixing ratio with pressure:

$$\frac{\partial q_s}{\partial p} = \frac{q_s RT}{p} (\varepsilon L - C_p T)\ (L^2 \varepsilon q_s + RC_p T^2)^{-1} \qquad (6.1.2)$$

We utilize the vertical displacement for determining whether saturation is reached, and thus

$k_1 = 1$ if $\omega < 0$ and $U > 1$ after vertical displacement.

otherwise $k_1 = 0$

The parameter k_2 is used to simulate the fact , that it takes some time for the droplets to grow, before precipitation starts to fall.

The time (t) the droplets spend in the cloud, assuming that they follow the air motion, can be estimated by

$$t = - \frac{g\rho}{\omega} (H_T - H_S) \qquad (6.1.3)$$

It is assumed that if $t < 300$ s no precipitation will form and that the rain will reach full intensity if $t > 1200$ s.

$$k_2 = 0 \quad t < 300 \text{ s}$$

$$k_2 = (t-300)/900 \quad 300 < t < 1200 \text{ s}$$

$$k_2 = 1 \quad t > 1200 \text{ s}$$

We also assume that $k_2 = 1$ if the air is saturated before the orographic uplift; i e if $U_0 > 1$.

6.2 Coalescence

A layer of air producing precipitation, also contains cloud droplets. When rain from a layer above falls through this layer, the precipitation production is enhanced by coalescence. In order to parameterize this effect we do the following assumptions:

i) 10% of the condensate is cloud water

ii) The condensation takes place at U = 90%

iii) All cloud droplets have a radius of 10 µm

Thus the cloud water density, q_w, (kg m^{-3}) is given by

$$q_w = 0.1\ (U - 0.9) \cdot q_s \cdot \rho \qquad (6.2.1)$$

where U is the relative humidity after the vertical displacement.

Now it is assumed that the precipitation intensity in a layer j, is enhanced by washout from the layer above j+1. Thus the precipitation rate is given by P^j =

$P_1{}^j + P_2{}^j$ where $P_1{}^j$ is given by (6.1.1) and

$P_2{}^j = f\ (P^{j+1}, q_w{}^j)$

For computing coalescence we must utilize information about rain drop spectrum, fall velocities etc.

The increase in intensity by washout is $P_2{}^j = W \cdot \Delta Z$, where ΔZ is the layer thickness and

$$W = q_w \int_0^\infty N(a) \cdot V(a) \cdot E(a) \cdot \pi\, a^2\, da \qquad (6.2.2)$$

Here N(a) is the rain drop spectrum (a = radius)

V(a) is the fall velocity, which is also dependent on the density of the surrounding air.

$E(a)$ is the coalescence efficiency (Actually E is also dependent on the cloud drop size but we assume that all cloud droplets have a radius of 10 μm).

We have utilized the rain drop distribution given by Best (see Mason, 1971, page 608), which is related to the precipitation rate:

$$F(a) = 1 - \exp\left[-\left(\frac{a}{\alpha P^{\beta}}\right)^{n}\right] \tag{6.2.3}$$

Where $F(a)$ is the part of the rain drop mass for rain drops with a radius less than a. P is the precipitation rate and the values of the constants are:

$$\alpha = 4{,}344 \cdot 10^{-3}, \ \beta = 0{,}232, \ n = 2{,}25$$

The rainwater concentration, M, is given by

$$M = 0{,}0737 \cdot P^{0.85} \ \mathrm{kg\ m^{-3}} \tag{6.2.4}$$

(Mason, 1971, page 610)

Utilizing the formulae given above we can write

$$N(a) = \tfrac{4}{3}\pi a^{3} \cdot \rho_w \cdot da = M \cdot \frac{\partial F}{\partial a} \cdot da \tag{6.2.5}$$

where ρ_w is the density of water

(6.2.5) and (6.2.2) give

$$W = \frac{q_w \cdot M \cdot 3}{4 \cdot \rho_w} \int_0^{\infty} \frac{1}{a} \frac{\partial F}{\partial a} \cdot V(a) \cdot E(a)\, da \tag{6.2.6}$$

$V(a)$ and $E(a)$ are taken from Mason, 1971 (PP 594, 598, 580).

We also assume that the precipitation after coalescence cannot exceed that of (6.1.1) with both k_1 and k_2 equal to unity.

6.3 Evaporation of rain drops in unsaturated layers

It was found by Best (1952) that rain drops changed their radii by evaporation when falling from Z_1 to Z_2 in a relative humidity, U, according to

$$a_1^2 - a_2^2 = A\left(e^{-\alpha Z_2} - e^{-\alpha Z_1}\right)(1 - U)^{1.13} \tag{6.3.1}$$

where a_1 and a_2 are the radii at heights Z_1 and Z_2 respectively.

$A = 1.375 \cdot 10^{-6}$ and $\alpha = 2.9 \cdot 10^{-4}$.

Knowing the precipitation rate before evaporation, we can compute the rain drop spectrum, and by integration over all rain drops we can derive a new spectrum, utilizing formula (6.3.1). This in turn can be interpreted as a new precipitation rate, after evaporation.

6.4 Incorporation of coalescence and evaporation in the model

The effects of coalescence and evaporation are included in the model according to the following algorithm;

What we shall modify is P_1^j, i e the precipitation production of each layer j, as given by (6.1.1). Denote the highest level, at which precipitation is formed by ℓ, $(P_1^\ell = P^\ell)$. If $P^{\ell-1}$ is non-zero it is modified, by use of (6.2.6) i e

$$P^{\ell-1} = P_1^{\ell-1} + P_2^{\ell-1} = P_1^{\ell-1} + f\,(P_1^\ell, q_w{}^{\ell-1}) \qquad (6.4.1)$$

also check that $P^{\ell-1} < P_{1max}^{\ell-1}$

$(P_1^{\ell-1}$ with both k_1 and k_2 equal to unity)

If also the next lower level is saturated utilize (6.4.1) again

$$P^{\ell-2} = P_1^{\ell-2} + f\,(P^{\ell-1},\ q_w{}^{\ell-2}) \qquad (6.4.2)$$

when entering an unsaturated layer, say ℓ-3 we utilize (6.3.1) for all precipitation falling through this layer i.e.

$$P_E^k = P^k - E^k \quad \text{for } k = \ell,\ \ell-1,\ \ell-2 \qquad (6.4.3)$$

We then continue down in the model atmosphere utilizing (6.4.1) and (6.4.3) until we reach the lowest layer. Thereafter we have a new vector P_E^j giving the modified precipitation intensity in each layer, which then is summed up as precipitation.

Bell (1978) included the effect of precipitation drift by the wind. He also smoothed the precipitation pattern after the forecast, to parameterize a horizontal coupling of the dynamics. This has not been done in this study.

7. EXPERIMENTS AND RESULTS

7.1 The test area

We have tested this model on the drainage basin of the lake Kultsjön, which is situated in the south of Lappland in Sweden, near the border to Norway. The computation grid consisted of 16x11 points. When utilizing the more complex vertical velocity formula (5.2.3) we used a somewhat larger area (19x15 points), since the SAM includes the effects of horizontally coupled fields, and we want to avoid boundary effects. The horizontal resolution is about 5 km (Δx = 5004 m, Δy = 4632 m). Figure 3 shows the orography and the drainage divide.

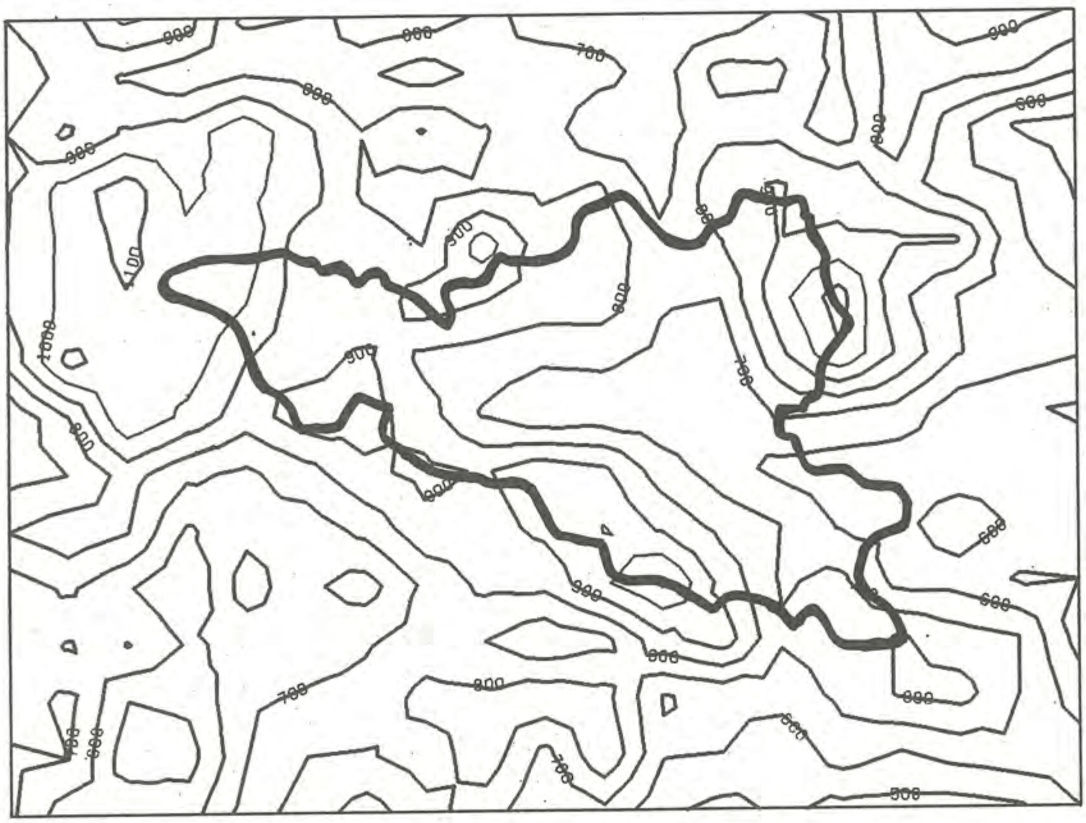

Figure 3 The orography and the drainage basin of Kultsjön

7.2 Experiments

We utilized the Swedish LAM (Undén, 1982) as input with forecasts valid every third hour from +12h to +36h. The model was run once a day from the LAM forecast starting at 18Z. Examples of forecasts are shown in Figure 4. The first picture (Fig 4a) shows the precipitation result when utilizing the simple formula (5.2.2) (A somewhat smaller area was used at that time, see 7.1), and Figure 4b depicts the same, but here we have utilized the more refined vertical velocity (5.2.3).

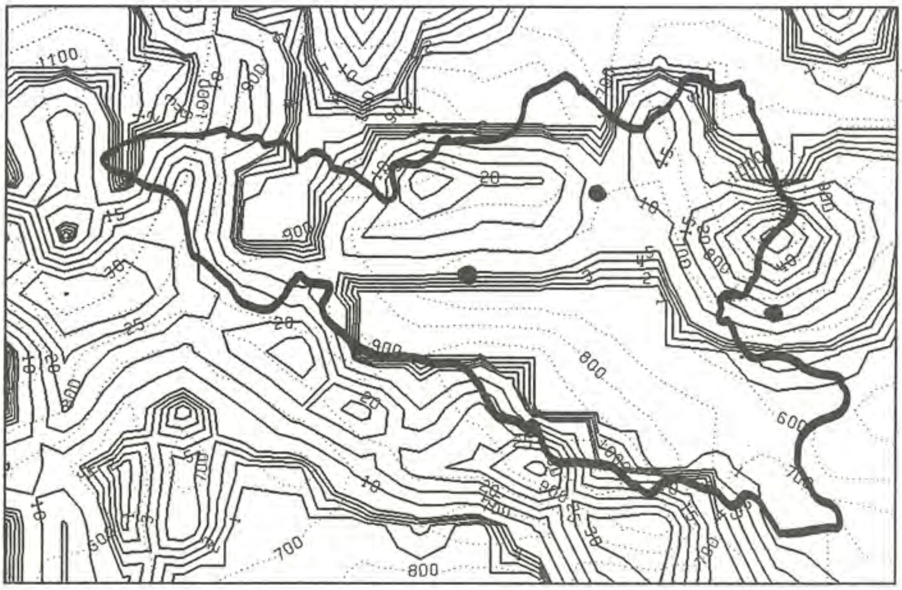

Figure 4a Accumulated 24h precipitation from a 36h forecast starting at 830931 at 18z. The vertical velocity is given by (5.2.2) The big dots indicate stations with precipitation measurements. The orography is shown as dotted lines.

Figure 4b The same as 4a, but the vertical velocity is given by (5.2.3)

The gradients are sharper in the first case. Over the same horizontal distance we have precipitation from zero to about 60 mm on Fig 4a and only to about 30 mm on Fig 4b. (The maxima to the right, on the border of the drainage basin). The areal means of the two examples in Fig 4 are 7,9 mm (4a) and 4,8 mm (4b).

It is a very difficult problem to verify areal mean values of precipitation. We have for this area only three stations. They are marked with dots on Figure 4a. They are all situated near the lake, and hence at a relatively low level. We think that three stations are too few for verifying and that their location is not representative. However, that is what we have available at this stage. In Figure 5 we compare the areal mean from the model runs (using the vertical velocity formulation (5.2.3)) with a mean value of the three measurements. The test period is from August 1 to October 29, 1983.

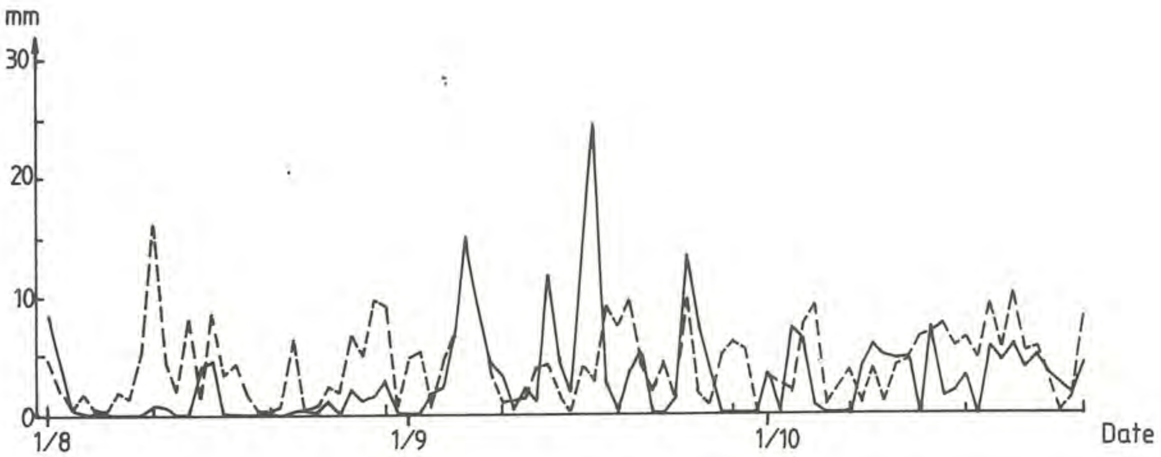

Figure 5 **24th precipitation.**
Solid line: Mean value of three observations
Dashed line: Forecast areal mean

Another way of verifying areal mean values has also been tested. We have utilized a hydrological runoff model available at SMHI (Bergström, 1976). One input to that model is the precipitation, as given by the mean value of the three available measurements. An estimation of the areal mean has then been done according to the actual orography, by using climatological corrections of the variation of precipitation with height.

Figure 6 shows the observed runoff ($m^3\ s^{-1}$) for the same period. This curve has some noise due to on the measure method. In Figure 7 we have the computed runoff, when utilizing the hydrological model, and the precipitation as measured by the three stations. One can see that there is a good agreement between the curves in Figures 6 and 7.

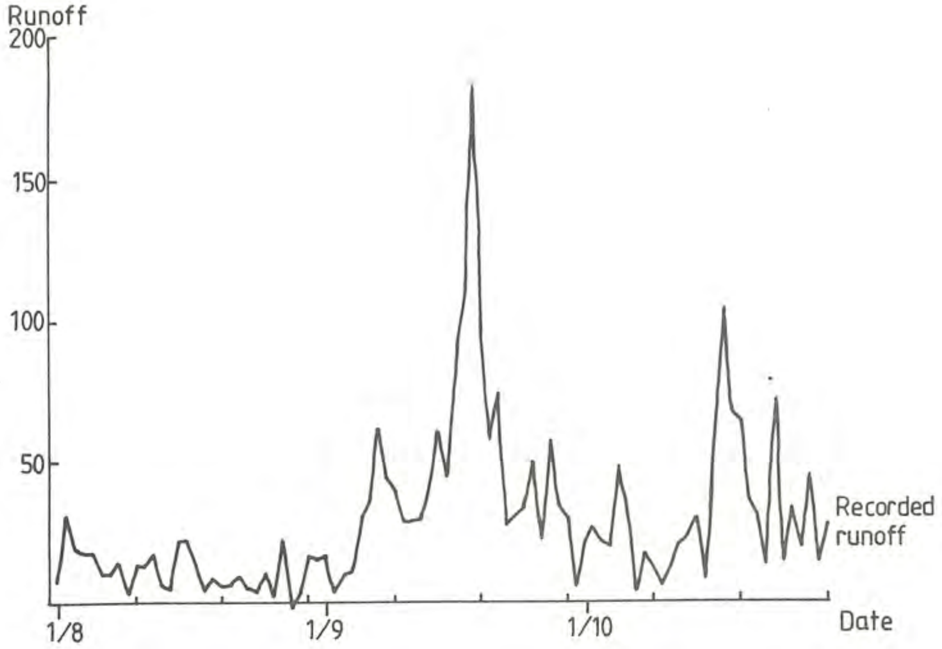

Figure 6 **Observed runoff (m^3 s^{-1})**

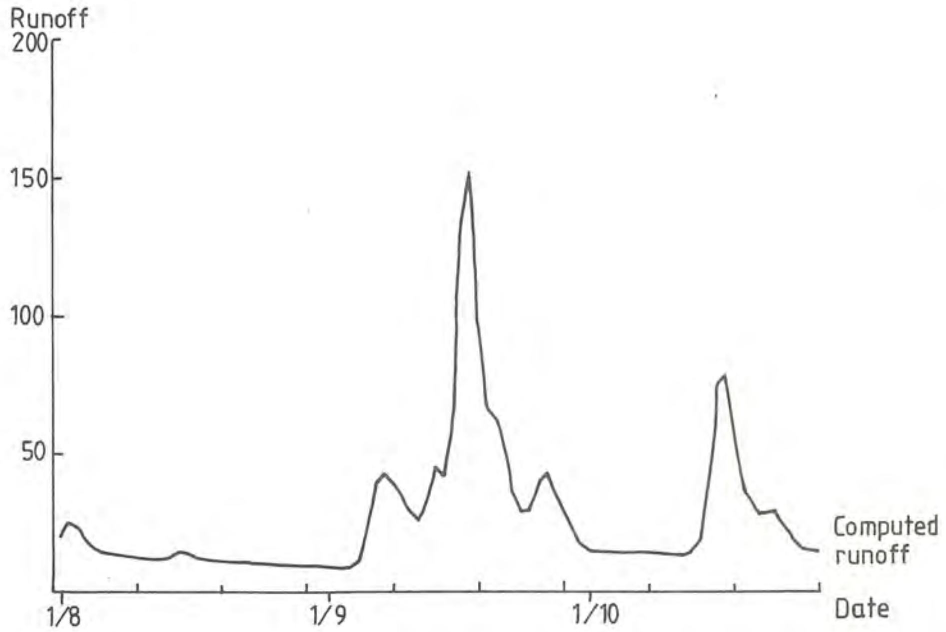

Figure 7 **Computed runoff using observed precipitation**

We have also computed the runoff by using the forecast areal mean precipitation, without the height correction mentioned above. The corresponding curves for the two different formulations of the vertical velocity are shown in Figure 8. In the first figure (8a) we utilized (5.2.2) and in the other (5.2.3) is used.

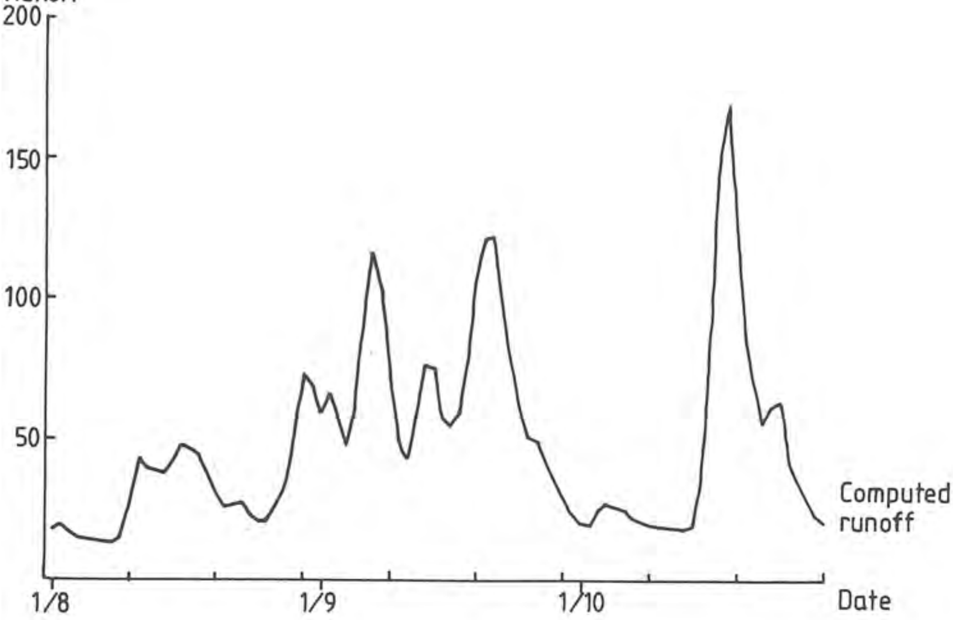

Figure 8a **Computed runoff, forecast precipitation using formula (5.2.2)**

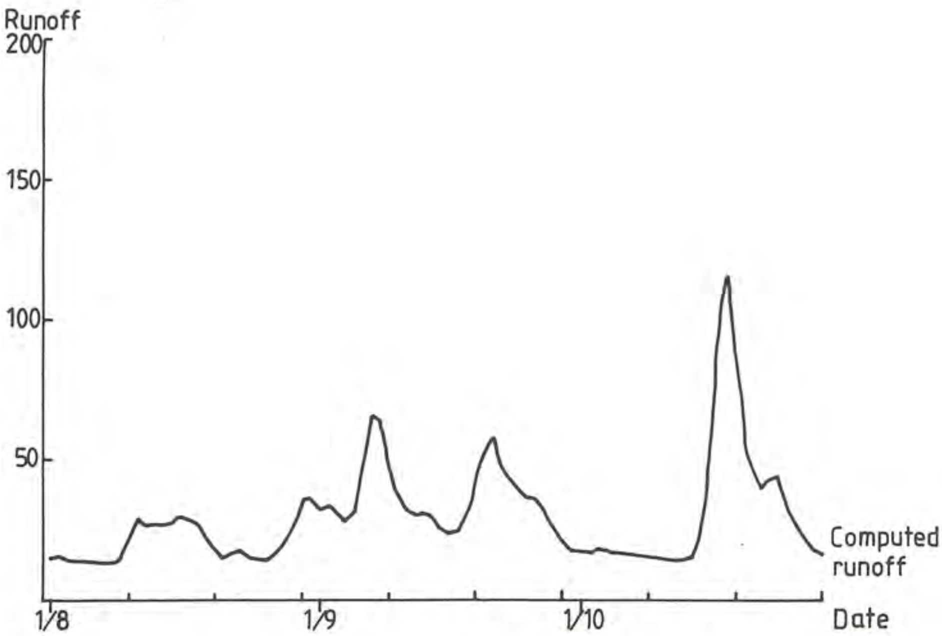

Figure 8b **The same as 8a but using (5.2.3)**

One can see that there is too much runoff in Figure 8a. The mean value is here 48,4 $m^3\ s^{-1}$, while the corresponding value of the observed runoff is 29,8 $m^3\ s^{-1}$. The mean value in Figure 8b is 30,0 $m^3\ s^{-1}$. The fact that the mean value is near the observed, indicates that our model in this version is climatologically reasonable. The peak in the middle of Figure 6 is missing in both 8a and 8b. On the 17th of September the forecast values were only a few millimeters in both methods, while the measured values were over twenty (see Figure 5).

A closer examination of this case, showed that the vast amount of precipitation came from a relatively small-scale cyclone, approaching from the south. The LAM-forecast of this case could not resolve that cyclone, but showed a less intensive (but good positioned) system. Our model approach cannot solve the problem of small-scale, not orographically induced, systems. The way this enters the model is by the term $\omega_{LAM}(p)$ in formula (5.2.3), which in this case was underestimated by the large-scale model. We hope that the evolution on ordinary NWP-models, with higher resolution will, at least partly, solve this problem.

We have also made some experiments to examine the usefulness of this precipitation model for runoff computations, using the existing hydrological model. When computing the runoff, we should not utilize the accumulated errors of the precipitation forecasts, but instead use the observations up to the actual forecast time. Therefore the following experiment was performed:

The runoff model was run once a day, with the observed precipitation as input, but on every run changing the last value to the corresponding forecast value (Figure 5). Here we have applied the height corrections (see above) only to the observed precipitation. The computed runoff from each run is shown in Figure 9.

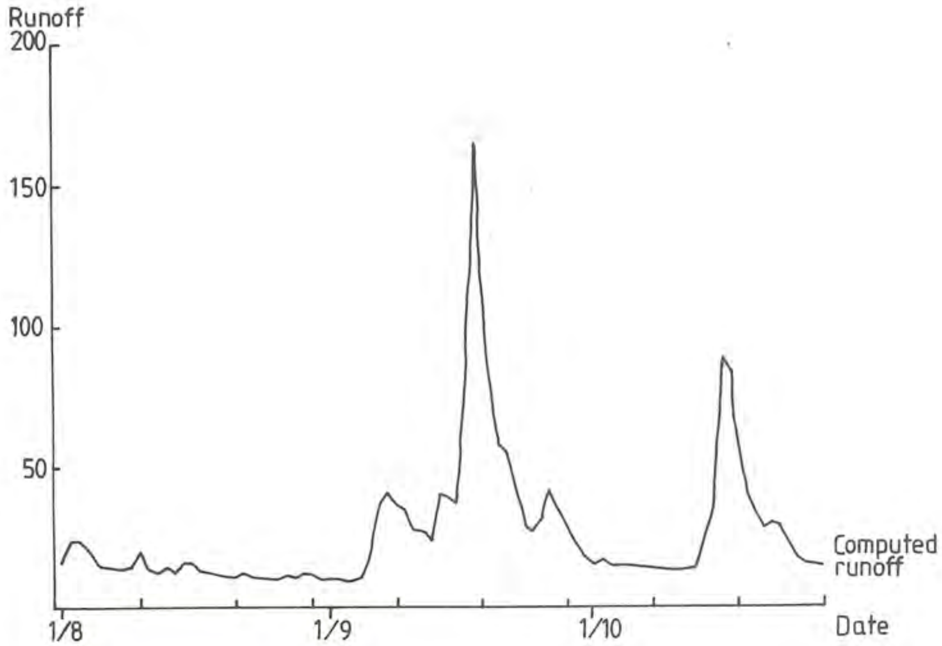

Figure 9 **Computed runoff using both observed and forecast precipitation (see text)**

The absolute values of the difference between the curves of Figure 9 and Figure 7 (i e the runoff error due to the use of predicted precipitation, instead of observed) is depicted in Figure 10. The most predominant feature is the effect of the erroneous forecast discussed above. To get an idea of how large these errors are we have also performed the same experiment utilizing a climatological (i e a mean value over the test period) value (~ 3 mm) of the precipitation instead of our predicted values. The corresponding errors are shown in Figure 11. Here the values are comparable to those of Figure 10, indicating the following:

i) Our precipitation model does not give any extra skill to the runoff computations, over that of climatology.

ii) The runoff model is very much dependent on the history and it is not very sensitive to the last precipitaion value, at least in this test area.

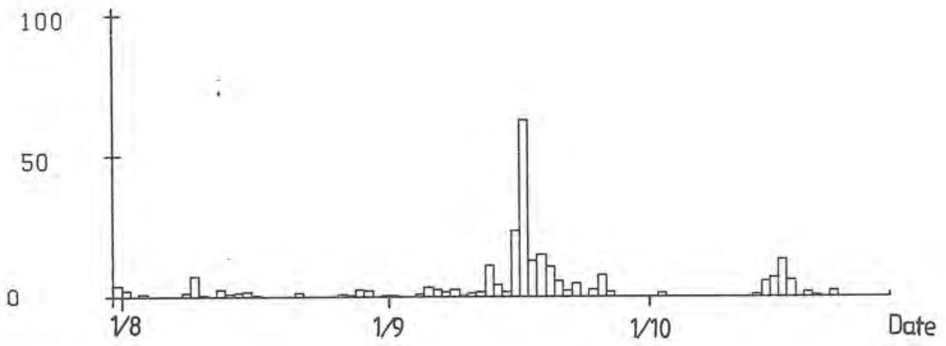

Figure 10 Absolute value of runoff error due to forecast precipitation instead of observed

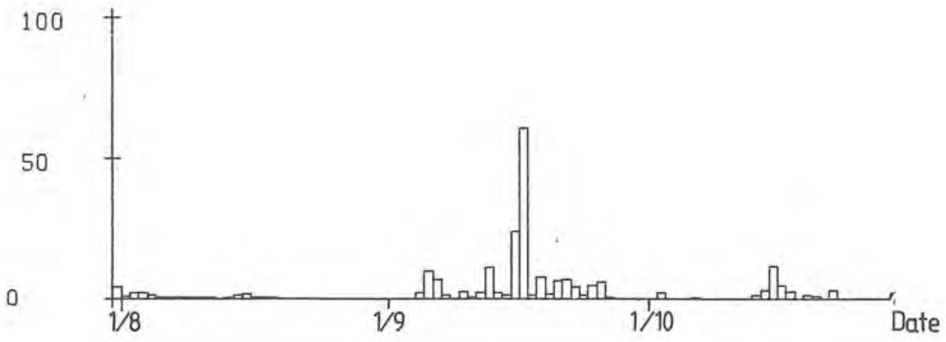

Figure 11 Absolute value of runoff error due to climatological precipitation instead of observed

Thus, the question of how to verify precipitation forecasts can only partly be answered utilizing a runoff model of this kind.

The main conclusion from these experiments is that over a three month period there are no systematic errors in the areal mean precipitation forecasts, but the quality of the individual forecasts varies from case to case.

In this study we have not used any explicit parameterization of convection. However, the convection is positively correlated to the vertical displacement and the vertical velocity, and since the precipitation rate is a function of these effects, one can regard the convection as included in the model. A more refined convection scheme would utilize a small-scale heating of the ground and a small-scale humidity field, which is difficult to extract from a large-scale model.

By this dynamical approach for precipitation forecasts, we get not only areal means, but also spatial distributions of the precipitation. This can, of course, be utilized for runoff computations in more complex hydrological models. For good verifications, however, an extensive network of precipitation meters is needed.

8. SUMMARY AND CONCLUSIONS

We have developed a dynamical model for computing orographic precipitation on the meso-scale. In doing so we have assumed that the flow on this scale can be regarded as an interpretation of the flow on the larger scale, the latter given by a synoptic numerical model forecast. Two methods of estimating the steady state vertical velocity have been used. The simplest vertical velocity is proportional to the horizontal wind and the local gradient of orography. To allow for a horizontal coupling of the flow, we have also used a two-dimensional model for computing the divergence in the lowest layer and hence the vertical velocity. This has then been used as a lower boundary condition in the second estimation of the vertical velocity.

The results show that the amount of precipitation is very sensitive to the formulation of the vertical velocity. When using the more physical formulation of the vertical velocity, we have found, by aid of a hydrological runoff model, that the precipitation over a three month period is climatologically reasonable. We think that future work in this field should be focused on the dynamical part, i e the estimation of the small-scale vertical velocity.

A very important problem is that of the verification. Due to a very limited number of measure stations, the areal mean value of the precipitation, computed from these has only limited value. The verification using the runoff model is only partly successful and we believe that an extensive network of measure stations is needed for future development of this type of precipitation models.

We have also examined the practical usefulness of the present model for use together with the existing runoff model. During the test period, no extra skill in the runoff computations by using forecast precipitation instead of climatology, is reached. We think, however, that this dynamical approach, giving not only areal means, but also spatial distributions, is a step in the right direction for solving the complex problem of precipitation forecasting.

9. ACKNOWLEDGEMENT

This project has been financed by the Swedish Association of River Regulation Enterprises, VASO (= Vattenregleringsföretagens samarbetsorganisation). For valuable discussions, I want to thank my colleagues at the Meteorological Research Department of SMHI, especially Esbjörn Olsson, Per Kållberg and Håkan Törnevik. I also want to thank Göran Sandberg, Sten Bergström and Magnus Persson, SMHI, for discussions about the runoff model.

10. REFERENCES

Bell, R. S., 1978: The forecasting of orographically enhanced rainfall accumulations using 10-level model data. Met. Magazine, 107, pp 113-124.

Best, A. C., 1952: The evaporation of rain drops. Q.J.R. Met. Soc., 78, pp 200-225.

Businger, J.A. et al., 1971: Flux-profile relationship in the atmospheric surface layer. J. Atmos. Sci., 28, pp 181-189.

Danard, M., 1977: A simple model for mesoscale effects of topography on surface winds. Month. Weath. Rew., 105, pp 572-581.

Olsson, E., 1984: Dynamic simulation of surface winds. Proceedings on simplified dynamical models for short-range forecasting on the mesoscale. R & D-notes no 37. SMHI.

Paulsson, C. A., 1970: The mathematical representation of wind speed and temperature profiles in the unstable atmospheric surface layer. J. Appl. Met., 9, pp 857-861.

Sundqvist, H., 1981: Prediction of stratiform clouds: Results from a 5-day forecast with a global model Tellus 33, pp 242-253.

Undén, P., 1982: The Swedish limited area model RMK 35, SMHI.

SMHI
HO
kuy/L/SCR

SMHI Rapporter, METEOROLOGI OCH KLIMATOLOGI (RMK)

Nr 1 Thompson, T, Udin, I, and Omstedt, A
Sea surface temperatures in waters surrounding Sweden
Stockholm 1974

Nr 2 Bodin, S
Development on an unsteady atmospheric boundary layer model.
Stockholm 1974

Nr 3 Moen, L
A multi-level quasi-geostrophic model for short range weather predictions
Norrköping 1975

Nr 4 Holmström, I
Optimization of atmospheric models
Norrköping 1976

Nr 5 Collins, W G
A parameterization model for calculation of vertical fluxes of momentum due to terrain induced gravity waves
Norrköping 1976

Nr 6 Nyberg, A
On transport of sulphur over the North Atlantic
Norrköping 1976

Nr 7 Lundqvist, J-E, and Udin, I
Ice accretion on ships with special emphasis on Baltic conditions
Norrköping 1977

Nr 8 Eriksson, B
Den dagliga och årliga variationen av temperatur, fuktighet och vindhastighet vid några orter i Sverige
Norrköping 1977

Nr 9 Holmström, I, and Stokes, J
Statistical forecasting of sea level changes in the Baltic
Norrköping 1978

Nr 10 Omstedt, A, and Sahlberg, J
Some results from a joint Swedish-Finnish sea ice experiment, March, 1977
Norrköping 1978

Nr 11 Haag, T
Byggnadsindustrins väderberoende, seminarieuppsats i företagsekonomi, B-nivå
Norrköping 1978

Nr 12 Eriksson, B
Vegetationsperioden i Sverige beräknad från temperaturobservationer
Norrköping 1978

Nr 13 Bodin, S
En numerisk prognosmodell för det atmosfäriska gränsskiktet grundad på den turbulenta energiekvationen
Norrköping 1979

Nr 14 Eriksson, B
Temperaturfluktuationer under senaste 100 åren
Norrköping 1979

Nr 15 Udin, I, och Mattisson, I
Havsis- och snöinformation ur datorbearbetade satellitdata - en modellstudie
Norrköping 1979

Nr 16 Eriksson, B
Statistisk analys av nederbördsdata. Del I. Arealnederbörd
Norrköping 1979

Nr 17 Eriksson, B
Statistisk analys av nederbördsdata. Del II. Frekvensanalys av månadsnederbörd
Norrköping 1980

Nr 18 Eriksson, B
Årsmedelvärden (1931-60) av nederbörd, avdunstning och avrinning
Norrköping 1980

Nr 19 Omstedt, A
A sensitivity analysis of steady, free floating ice
Norrköping 1980

Nr 20 Persson, C och Omstedt, G
En modell för beräkning av luftföroreningars spridning och deposition på mesoskala
Norrköping 1980

Nr 21 Jansson, D
Studier av temperaturinversioner och vertikal vindskjuvning vid Sundsvall-Härnösands flygplats
Norrköping 1980

Nr 22 Sahlberg, J and Törnevik, H
A study of large scale cooling in the Bay of Bothnia
Norrköping 1980

Nr 23 Ericson, K and Hårsmar, P-O
Boundary layer measurements at Klockrike. Oct. 1977
Norrköping 1980

Nr 24 Bringfelt, B
A comparison of forest evapotranspiration determined by some independent methods
Norrköping 1980

Nr 25 Bodin, S and Fredriksson, U
Uncertainty in wind forecasting for wind power networks
Norrköping 1980

Nr 26 Eriksson, B
Graddagsstatistik för Sverige
Norrköping 1980

Nr 27 Eriksson, B
Statistisk analys av nederbördsdata. Del III. 200-åriga nederbördsserier
Norrköping 1981

Nr 28 Eriksson, B
Den "potentiella" evapotranspirationen i Sverige
Norrköping 1981

Nr 29 Pershagen, H
Maximisnödjup i Sverige (perioden 1905-70)
Norrköping 1981

Nr 30 Lönnqvist, O
Nederbördsstatistik med praktiska tillämpningar
(Precipitation statistics with practical applications)
Norrköping 1981

Nr 31 Melgarejo, J W
Similarity theory and resistance laws for the atmospheric boundary layer
Norrköping 1981

Nr 32 Liljas, E
Analys av moln och nederbörd genom automatisk klassning av AVHRR data
Norrköping 1981

Nr 33 Ericson, K
Atmospheric Boundary layer Field Experiment in Sweden 1980, GOTEX II, part I
Norrköping 1982

Nr 34 Schoeffler, P
Dissipation, dispersion and stability of numerical schemes for advection and diffusion
Norrköping 1982

Nr 35 Undén, P
The Swedish Limited Area Model (LAM). Part A. Formulation
Norrköping 1982

Nr 36 Bringfelt, B
A forest evapotranspiration model using synoptic data
Norrköping 1982

Nr 37 Omstedt, G
Spridning av luftförorening från skorsten i konvektiva gränsskikt
Norrköping 1982

Nr 38 Törnevik, H
An aerobiological model for operational forecasts of pllen concentration in th air
Norrköping 1982

Nr 39 Eriksson, B
Data rörande Sveriges temperaturklimat
Norrköping 1982

Nr 40 Omstedt, G
An operational air pollution model using routine meteorological data
Norrköping 1984

Nr 41 Christer Persson and Lennart Funkquist
Local scale plume model for nitrogen oxides.
Model description.

Nr 42 Stefan Gollvik
Estimation of orographic precipitation by dynamical interpretation of synoptic model data.

SMHI
HO
kuy/L/SCR

SMHI Rapporter, HYDROLOGI OCH OCEANOGRAFI (RHO)

Nr 1 Weil, J G
Verification of heated water jet numerical model
Stockholm 1974

Nr 2 Svensson, J
Calculation of poison concentrations from a hypothetical accident off the Swedish coast
Stockholm 1974

Nr 3 Vasseur, B
Temperaturförhållanden i svenska kustvatten
Stockholm 1975

Nr 4 Svensson, J
Beräkning av effektiv vattentransport genom Sunninge sund
Stockholm 1975

Nr 5 Bergström, S och Jönsson, S
The application of the HBV runoff model to the Filefjell research basin
Norrköping 1976

Nr 6 Wilmot, W
A numerical model of the effects of reactor cooling water on fjord circulation
Norrköping 1976

Nr 7 Bergström, S
Development and application of a conceptual runoff model
Norrköping 1976

Nr 8 Svensson, J
Seminars at SMHI 1976-03-29--04-01 on numerical models of the spreading of cooling water
Norrköping 1976

Nr 9 Simons, J, Funkquist, L and Svensson, J
Application of a numerical model to Lake Vänern
Norrköping 1977

Nr 10 Svensson, S
A statistical study for automatic calibration of a conceptual runoff model
Norrköping 1977

Nr 11 Bork, I
Model studies of dispersion of pollutants in Lake Vänern
Norrköping 1977

Nr 12 Fremling, S
Sjöisars beroende av väder och vind, snö och vatten
Norrköping 1977

Nr 13 Fremling, S
Sjöisars bärighet vid trafik
Norrköping 1977

Nr 14 Bork, I
Preliminary model studies of sinking plumes
Norrköping 1978

Nr 15 Svensson, J and Wilmot, W
A numerical model of the circulation in Öresund
Evaluation of the effect of a tunnel between Helsingborg and Helsingör
Norrköping 1978

Nr 16 Funkquist, L
En inledande studie i Vätterns dynamik
Norrköping 1978

Nr 17 Vasseur, B
Modifying a jet model for cooling water outlets
Norrköping 1979

Nr 18 Udin, I och Mattsson, I
Havsis- och snöinformation ur datorbearbetade satellitdata - en metodstudie
Norrköping 1979

Nr 19 Ambjörn, C och Gidhagen, L
Vatten- och materialtransporter mellan Bottniska viken och Östersjön
Norrköping 1979

Nr 20 Gottschalk, L och Jutman, T
Statistical analysis of snow survey data
Norrköping 1979

Nr 21 Eriksson, B
Sveriges vattenbalans. Årsmedelvärde (1931-60) av nederbörd, avdunstning och avrinning
Norrköping 1980

Nr 22 Gottschalk, L and Krasovskaia, I
Synthesis, processing and display of comprehensive hydrologic information
Norrköping 1980

Nr 23 Svensson, J
Sinking cooling water plumes in a numerical model
Norrköping 1980

Nr 24 Vasseur, B, Funkquist, L and Paul, J F
Verification of a numerical model for thermal plumes
Norrköping 1980

Nr 25 Eggertsson, L-E
HYPOS - ett system för hydrologisk positionsangivelse
Norrköping 1980

Nr 26 Buch, Erik
Turbulent mixing and particle distribution investigations in the Himmerfjärd 1978
Norrköping 1980

Nr 27 Eriksson, B
Den "potentiella" evapotranspirationen i Sverige
Norrköping 1980

Nr 28 Broman, B
On the spatial representativity of our oceanographic measurements
Norrköping 1981

Nr 29 Ambjörn, C, Luide, T, Omstedt, A, Svensson, J
En operationell oljedriftsmodell för norra Östersjön
Norrköping 1981

Nr 30 Svensson, J
Vågdata från svenska kustvatten 1979 - 1980
Norrköping 1981

Nr 31 Jutman, T
Stationsnät för vattenföring
Norrköping 1981

Nr 32 Omstedt, A, Sahlberg, J
Vertical mixing and restratification in the Bay of Bothnia during cooling
Norrköping 1982

Nr 33 Brandt, M
Sedimenttransport i svenska vattendrag
Norrköping 1982

Nr 34 Bringfelt, B
A forest evapotranspiration model using synoptic data
Norrköping 1982

Nr 35 Bhatia, P K, Bergström, S, Persson, M
Application of the distributed HBV-6 model to the Upper Narmada Basin in India
Norrköping 1984

Nr 36 Omstedt, A
A forecasting model for water cooling in the Gulf of Bothnia and Lake Vänern
Norrköping 1984

Nr 37 Gidhagen, L
Coastal Upwelling in the Baltic - a presentation of satellite and in situ measurements of sea surface temperatures indicating coastal upwelling
Norrköping 1984

SMHI

SWEDISH METEOROLOGICAL AND HYDROLOGICAL INSTITUTE
Box 923, S-601 19 Norrköping, Sweden. Phone +46 11 10 80 00. Telex 644 00 smhi s

ISSN 0347-2116